Table 1 Materials used.

Material	Notation	Properties
Cement	C	Ordinary Portland cement, density: 3.16g/cm^3, Blaine surface area: 3230cm^2/g
Fine aggregate	S	Ooi river sand, density at surface dry condition: 2.59g/cm^3, absorption: 2.08%
Coarse aggregate	GL	Limestone, density:2.64g/cm^3, absorption: 0.36%
	GS	Crushed sandstone, density:2.64g/cm^3, absorption:0.89%
Agent	AE	AE water reducing agent, polycarboxylic acid type
Agent	AS	Thickening agents, water-soluble cellulose type

Table 2 Chemical composition of cement.

	ig.loss	Chemical composition (mass%)								
	(%)	SiO_2	Al_2O_3	Fe_2O_3	CaO	MgO	SO_3	Na_2O	K_2O	Cl^-
N	2.3	20.04	5.21	2.87	64.9	1.46	2.21	0.14	0.34	0.019

Table 3 Mix proportions and fresh properties of concrete.

	Mixture proportion									Slump	Air	Temperature
	W/C	s/a	Mass (kg/m^3)							(cm)	(%)	(℃)
	(%)	(%)	W	C	S*	GL*	GS*	AE	AS			
LS	55	51.8	177	322	940	909	-	3	1.3	11.5	2.8	21
SS			177	322	940	-	892	3	1.3	9.5	2.5	21

* Aggregates are in the saturated surface dry condition.

Table 4 Physical properties of aggregate.

	Drying shrinkage from saturated state to 60% RH equilibrium [*1]	Bulk modulus[*2]
GL	-36 μ	71.1 GPa
GS	-230 μ	40.8 GPa

*1 Average of three orthogonal strains obtained with a thermal mechanical analyzer with a relative humidity generator (Bruker AXS, TMA4000SA + HC9700). Length-change isotherms are shown in the Appendix.

*2 Calculated using ultrasonic pulse velocity of P-wave and S-wave and density of aggregates. Average of three orthogonal values.

Table 5 Physical properties of materials assumed in the numerical analysis.

	Young's modulus E^* (N/mm^2)	Poisson's ratio (-)	Tensile strength f_t^* (N/mm^2)	Fracture energy G_{ft}^*(N/m)	Compressive strength f_c^* (N/mm^2)
Mortar	17	0.2	3.0	70[a)]	40
Aggregate	65	0.18	200[b)]	—[b)]	200[b)]
ITZ	[d)]	0.2[d)]	1.5, 2.25[c)]	7, 14, 35[c)]	40[d)]

a) Calculated from JSCE equation, b) aggregate failure is not assumed in the present calculation.

c) See Fig. 17, and Table 6, d) The same value as that of mortar is assumed.

Table 6 Applied values of springs in the numerical calculation.

(a) Normal spring

	Young's modulus	Tension field		Compression field			
	E (N/mm^2)	f_t (N/mm^2)	G_{ft} (N/mm)	f_c (N/mm^2)	ε_{c2}	α_{c1}	α_{c2}
Mortar	$1.3E^*$	$0.8f_t^*$	$0.5G_{ft}^*$	$1.5f_c^*$	-0.015	0.15	0.25
Aggregate							
ITZ							

(b) Shear spring

	Shear modulus	Failure criteria			Softening behavior			
	η=G/E	c (N/mm^2)	φ (degree)	σ_b (N/mm^2)	β_0	β_{max}	χ	κ
Mortar	0.4	$0.17f_c^*$	37	$0.5f_c^*$	-0.1	-0.05	-0.02	-0.6
Aggregate	0.35							
ITZ	0.4							

E^*, f_t^*, G_{ft}^*, f_c^* : shown in Table 5.

Table 7　Parameters of materials for drying process

	Volumetric water content at saturation w (10^{-3}g/mm^3)	BET surface area S (m^2/g)	Moisture transfer coefficient at saturation (mm^2/s・g/mm^3・(J/g)$^{-1}$)	Moisture capacity dw/du	Shrinkage at 60% RH	
					α_{sh}	
Mortar (=Paste)	0.2505	170	8.5×10^{-9}	0.0016	-1800 μ	
					4000×10^{-6}	
Aggregate	0.00765	10	8.5×10^{-8} a)	0.00005	-400 μ	0 μ
					906×10^{-6}	0
ITZ	0.129 b)	90 b)	8.5×10^{-8} a)	0.000825 b)	-1200 μ b)	-900 μ b)
					2450 $\times10^{-6}$ b)	2450 $\times10^{-6}$ b)

a): 10 times that of mortar, b):Average value of mortar and aggregate

Table 8 Notation and parameters for numerical analysis

Objective	Notation	Shrinkage of aggregate (μ)	Young's modulus of aggregate (GPa)	ITZ properties		
				Young's modulus E	Tensile strength f_t	Fracture energy G_{ft}
Simulation of concrete with sandstone and limestone	Sh0_E130_0.4Gft	0	130	$0.5E^*$	$0.5f_t^*$	$0.4G_{ft}^*$
	Sh400_E65_0.1Gft	400	65	$0.5E^*$	$0.5f_t^*$	$0.1G_{ft}^*$
Impact of Young's modulus and shrinkage of aggregate	Sh0_Ea65	0	65	$0.5E^*$	$0.5f_t^*$	$0.2G_{ft}^*$
	Sh0_Ea130		130			
	Sh400_Ea65	400	65			
	Sh400_Ea130		130			
Impact of Young's modulus and strength of ITZ	Sh0_0.5E_0.25f_t	0	65	$0.5E^*$	$0.25f_t^*$	$0.2G_{ft}^*$
	Sh0_0.5E_0.5f_t			$0.5E^*$	$0.5f_t^*$	
	Sh0_0.5E_0.75f_t			$0.5E^*$	$0.75f_t^*$	
	Sh0_0.5E_1.0f_t			$0.5E^*$	$1.0f_t^*$	
	Sh0_0.75E_0.25f_t			$0.75E^*$	$0.25E^*$	
	Sh0_0.75E_0.5f_t			$0.75E^*$	$0.5E^*$	
	Sh0_0.75E_0.75f_t			$0.75E^*$	$0.75f_t^*$	
	Sh0_0.75E_1.0f_t			$0.75E^*$	$1.0f_t^*$	
Impact of fracture energy of ITZ	Sh0_0.1Gft	0	65	$0.5E^*$	$0.5f_t^*$	$0.1G_{ft}^*$
	Sh0_0.2Gft					$0.2G_{ft}^*$
	Sh0_0.4Gft					$0.4G_{ft}^*$

E^*, f_t^*, G_{ft}^* : values for mortar shown in Table 5.

Fig. 1 Surface crack patterns of concrete with low-shrinkage limestone coarse aggregate (PL3-No.2) and high-shrinkage sandstone coarse aggregate (PL1-No.1) under uniaxial restraint conditions.

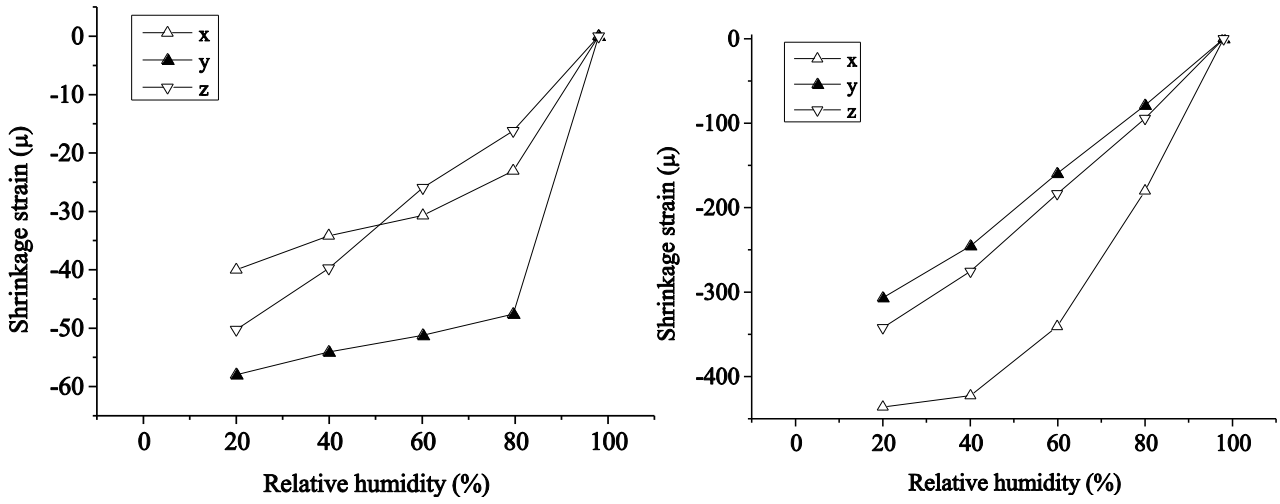

(a) GL (b) GS

Fig. 2 Short-term length-change isotherms of GL and GS.

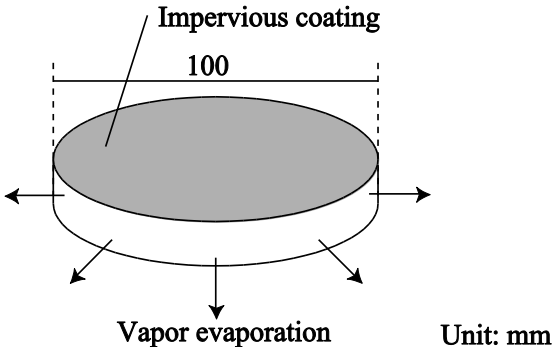

Fig. 3 Schematic of disk specimens

Fig. 4 System for capturing digital images of unrestricted shrinkage specimens [52].

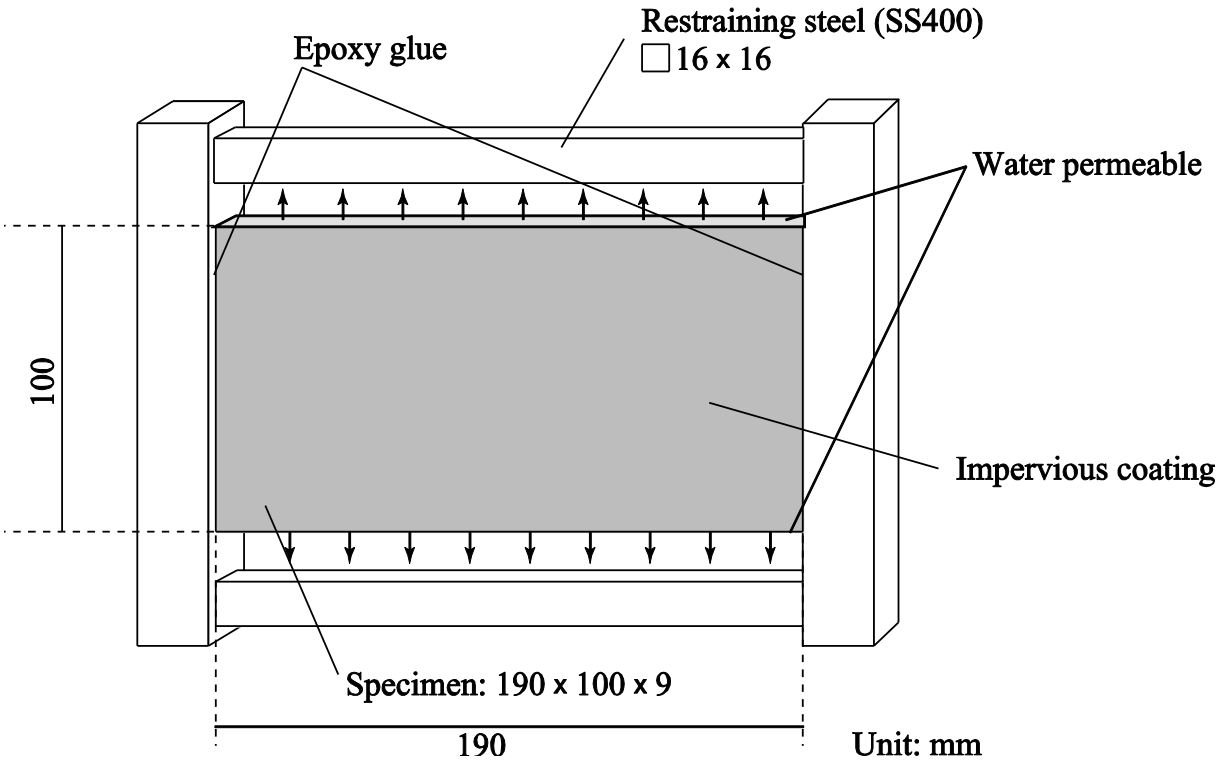

Fig.5 Schematic of restricted specimens

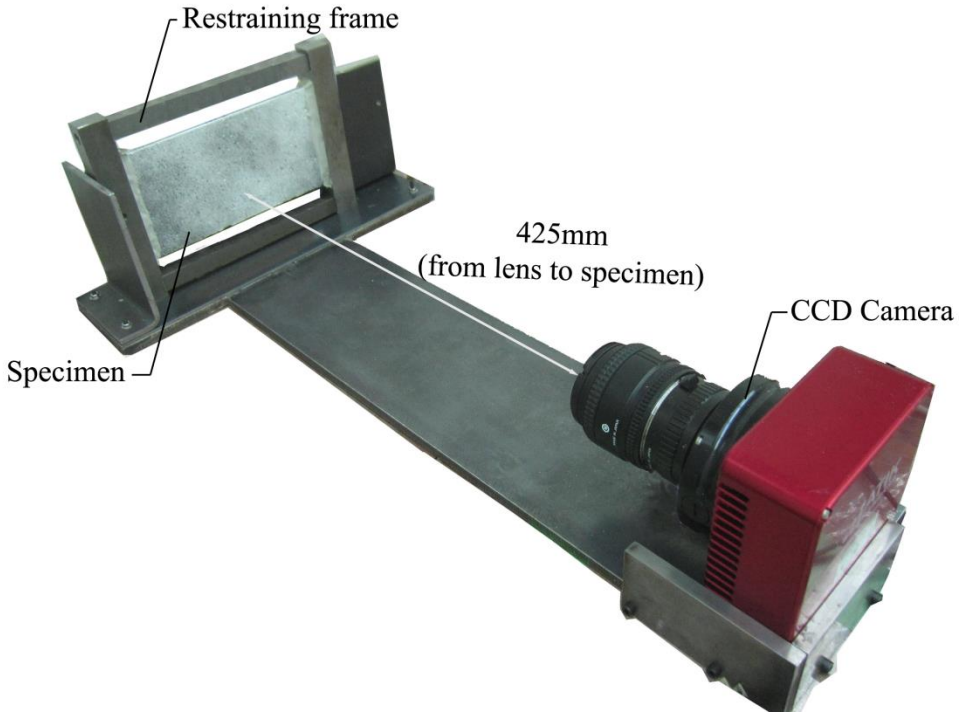

Fig. 6 System for taking digital images of restrained shrinkage specimens.

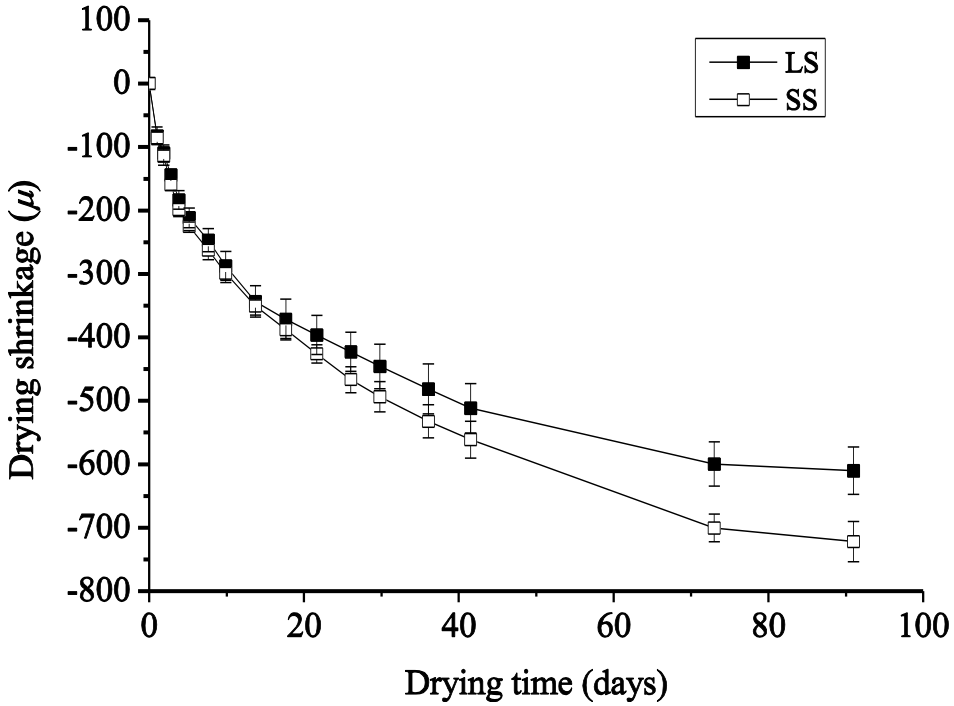

Fig. 7 Shrinkage of concretes. Error bars show 1-sigma.

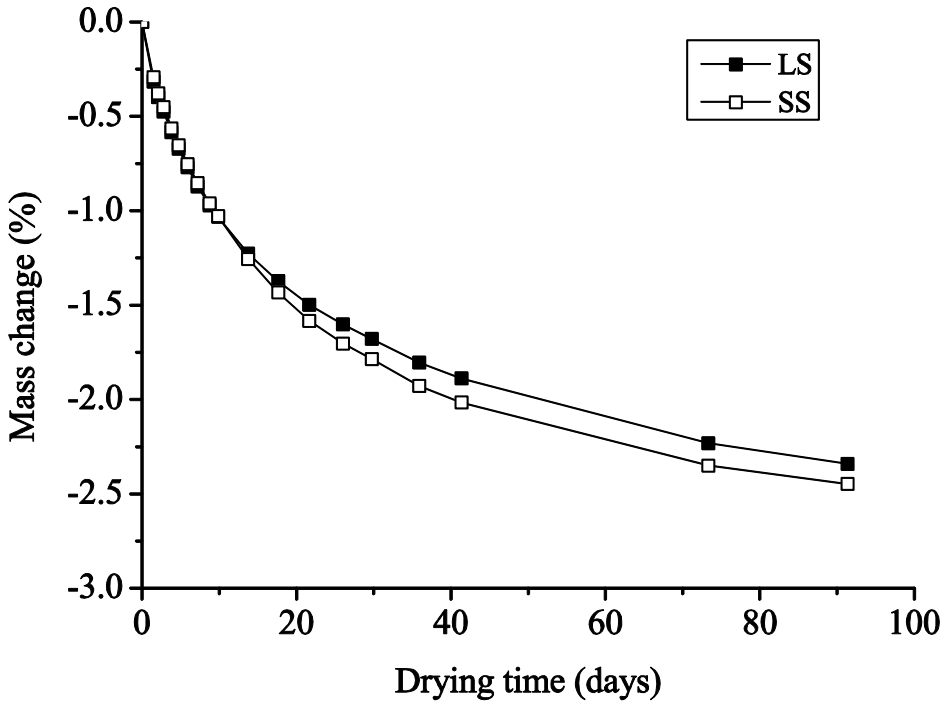

Fig. 8 Mass change of concretes. All the error bars for 1–sigma are within square plot.

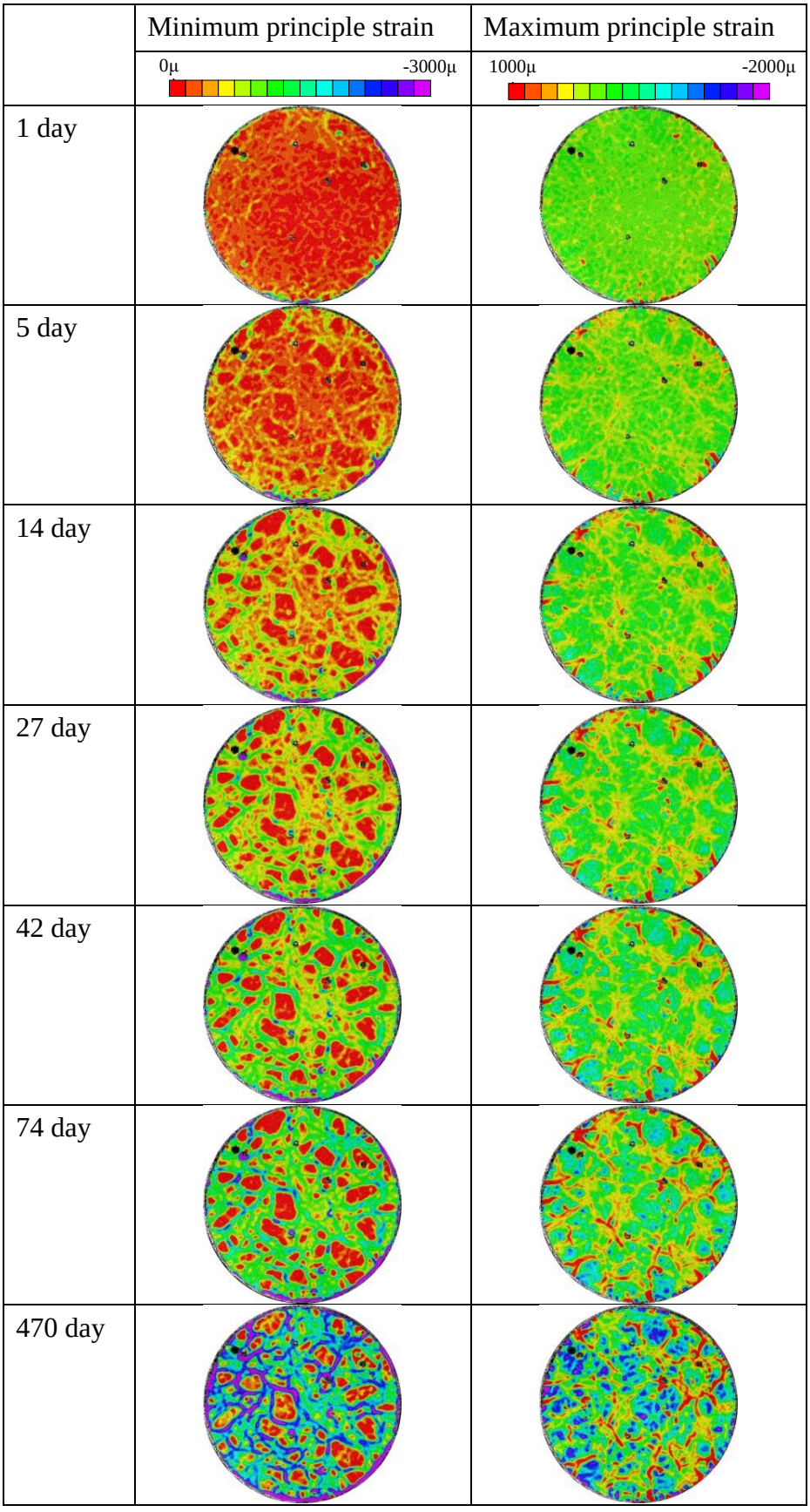

Fig. 9 Development of minimum and maximum strain distribution of LS sample section under drying using DICM.

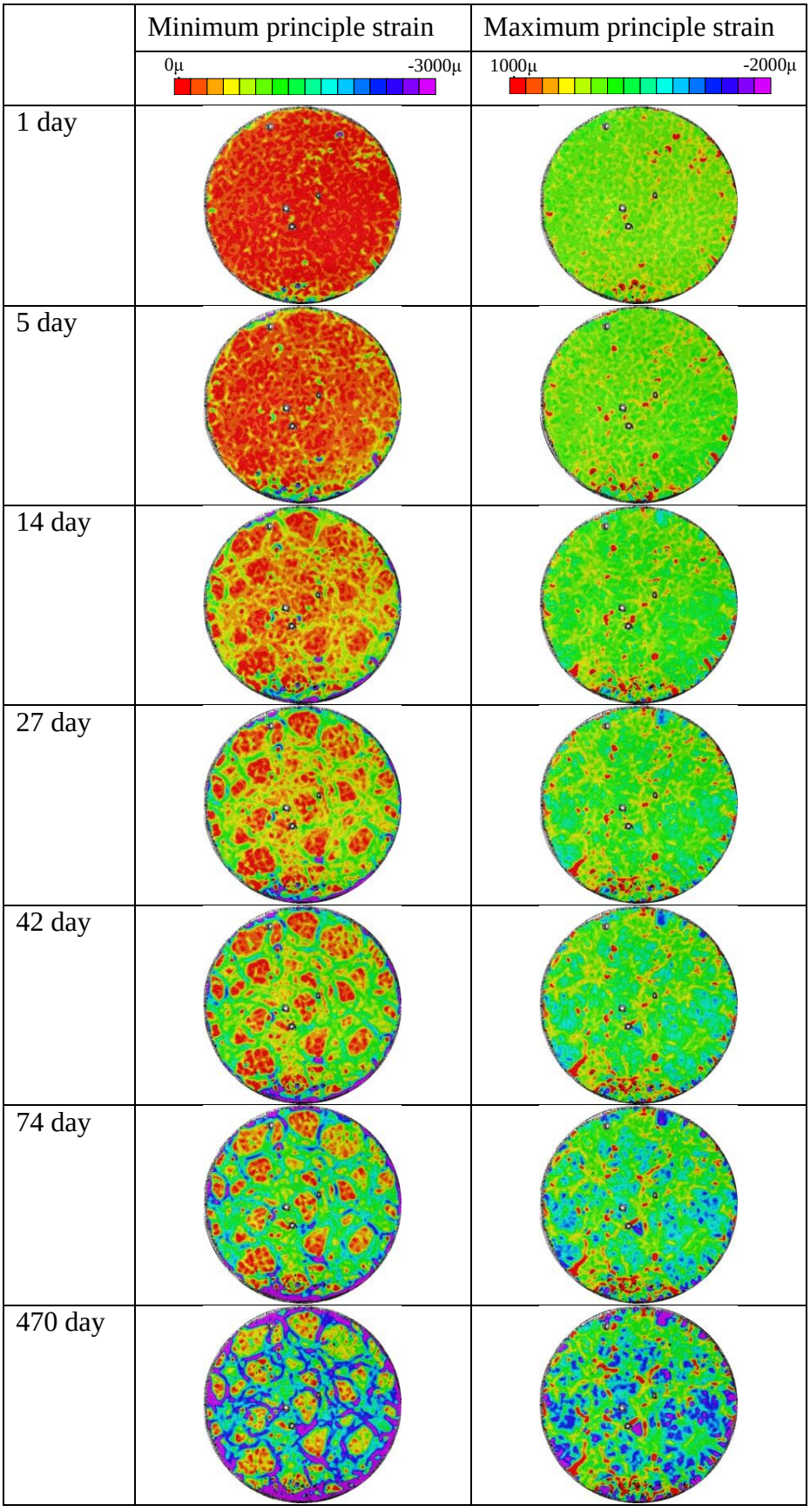

Fig. 10 Development of minimum and maximum strain distribution of SS sample section under drying using DICM.

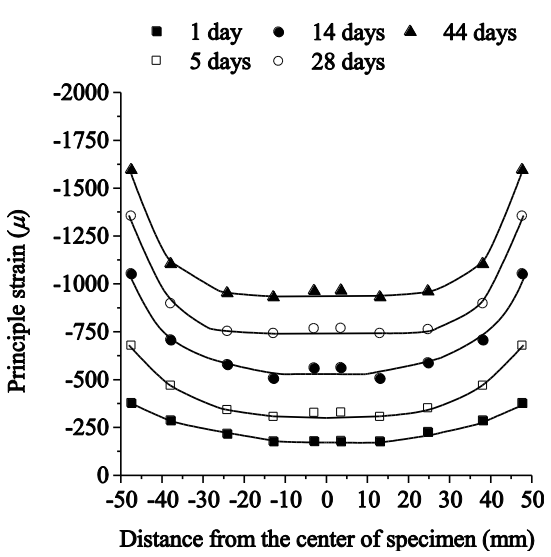

(a) LS

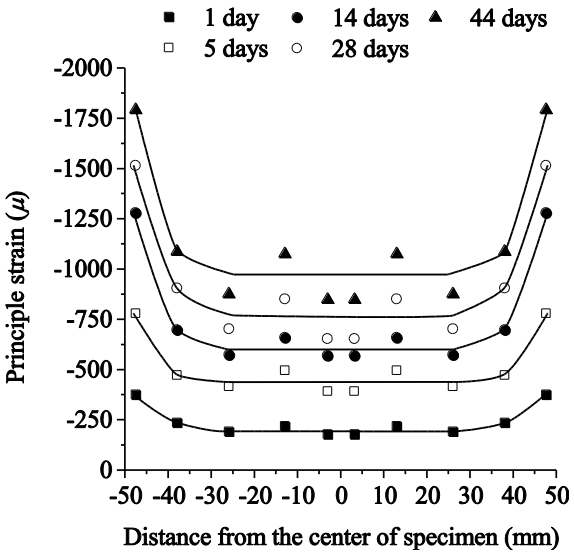

(b) SS

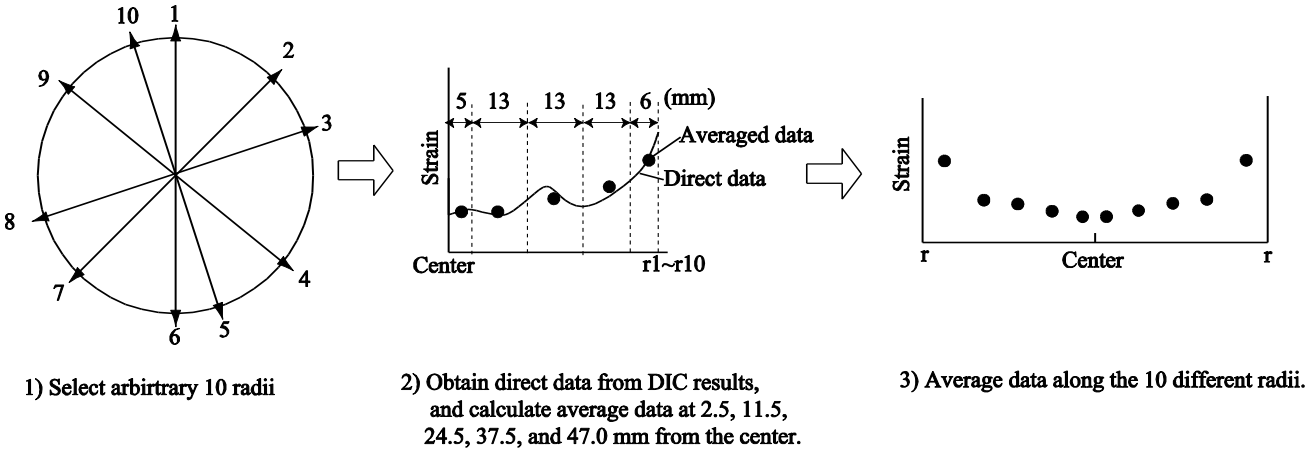

(c) Calculation procedure

Fig.11 Distribution of minimum principle shrinkage strain as a function of distance from the center of the specimen and drying periods. (a) LS, (b) SS, (c) Steps of data calculation.

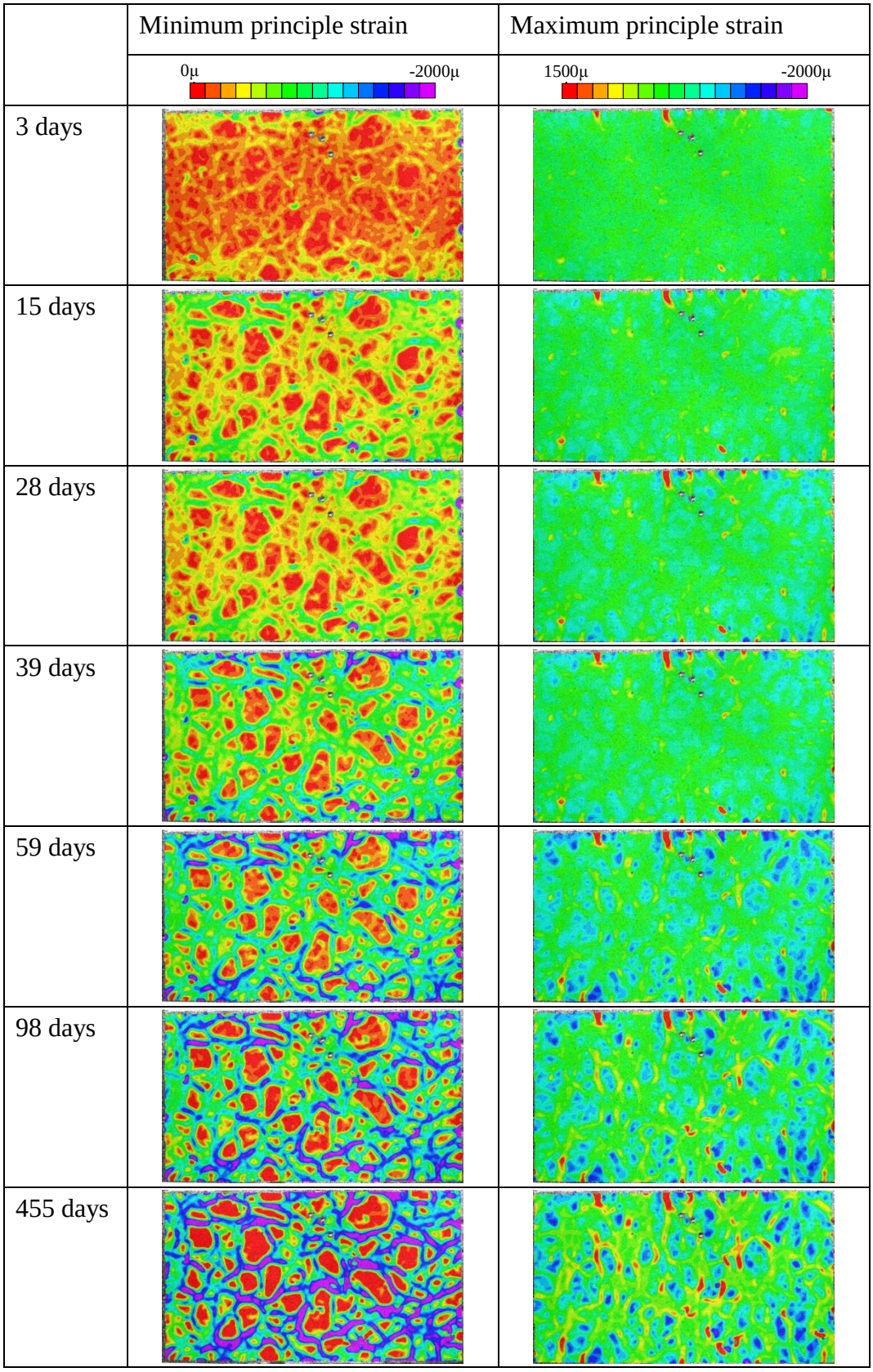

Fig. 12 Development of minimum and maximum principle strain distributions of restricted LS specimen during drying.

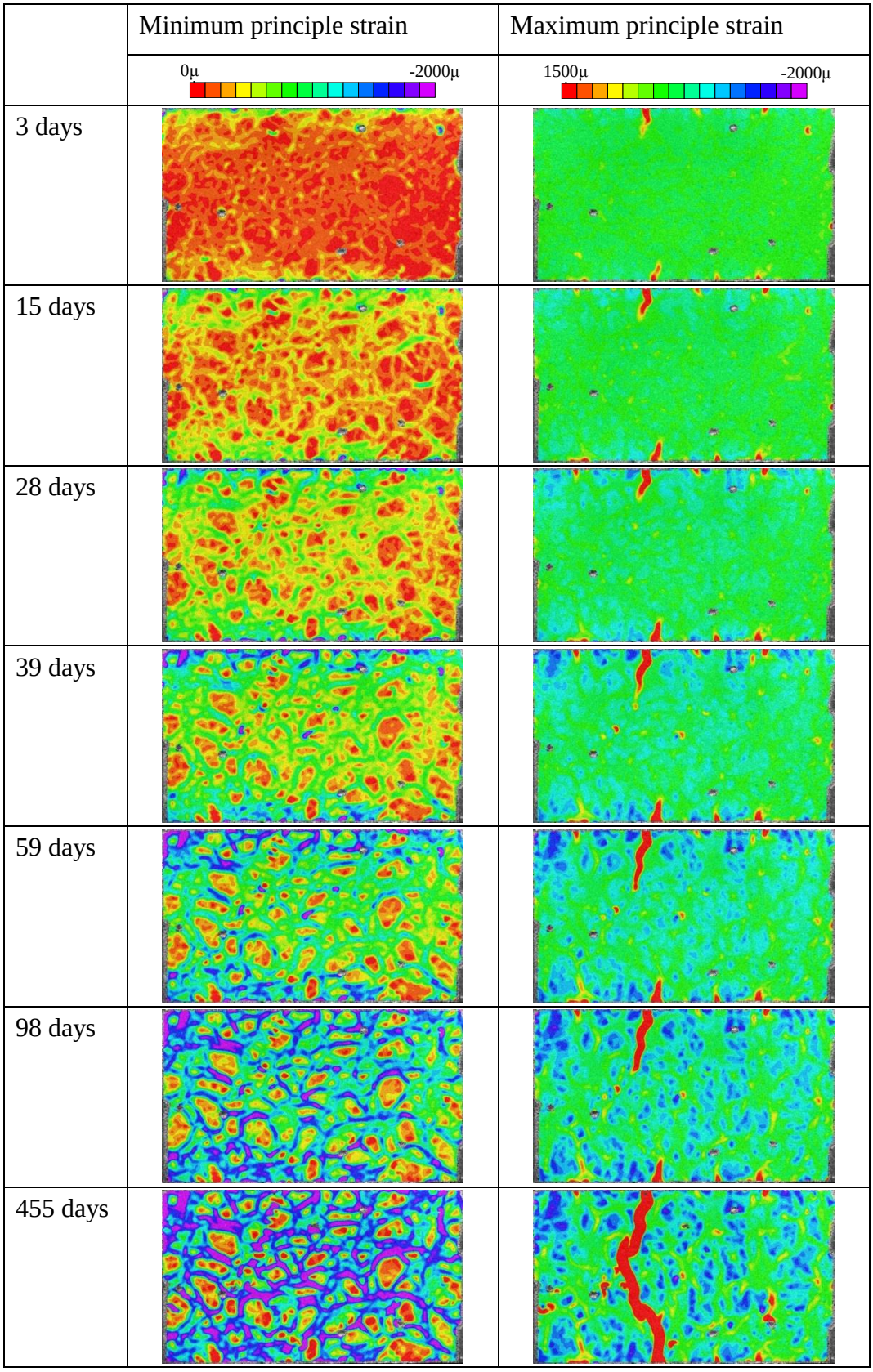

Fig. 13 Development of minimum and maximum principle strain distributions of restricted SS specimen during drying.

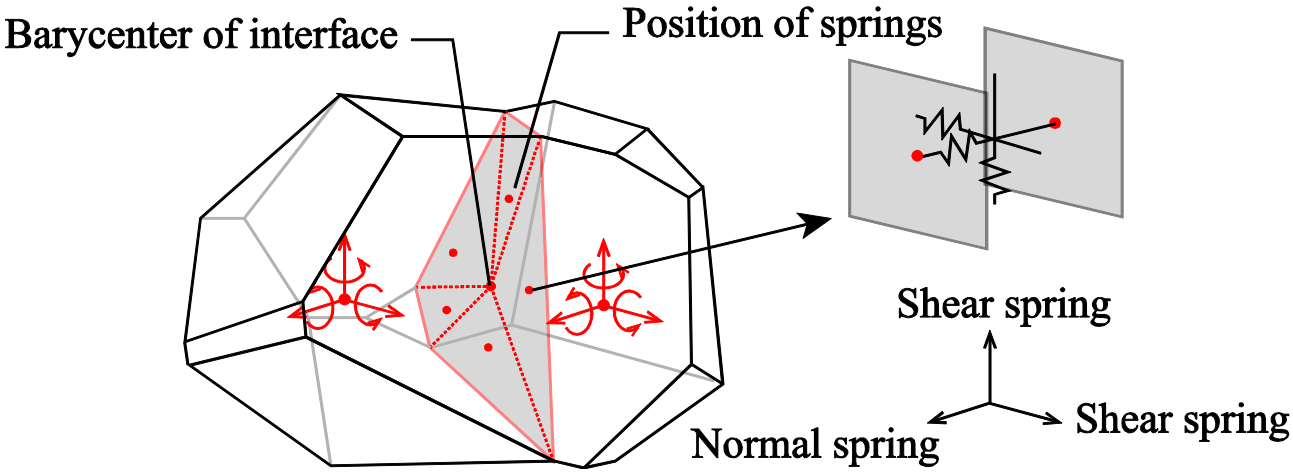

Fig. 14 Schematic of the elements in RBSM and springs connecting them.

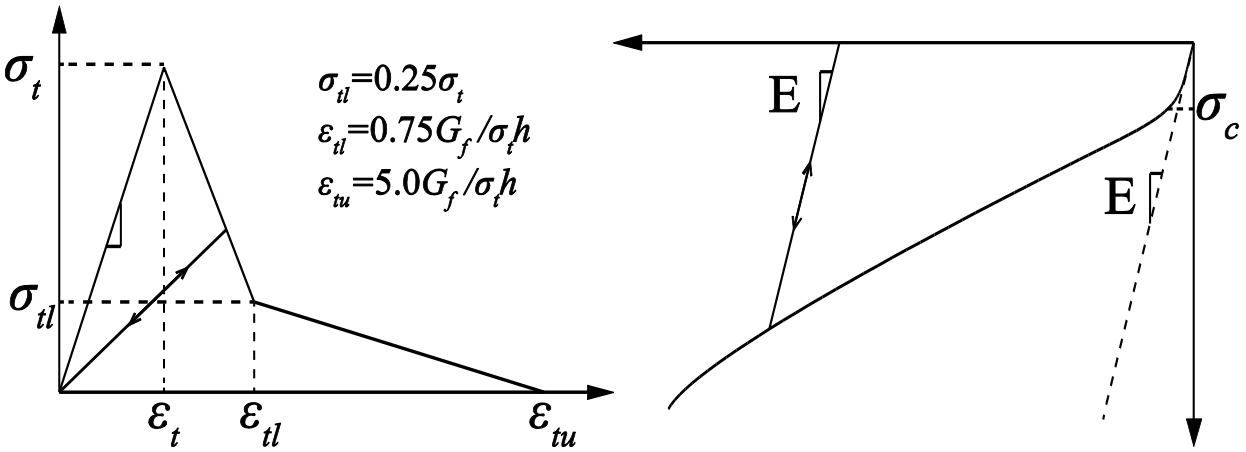

Fig. 15 Schematic of the constitutive low of the normal spring in the mortar.

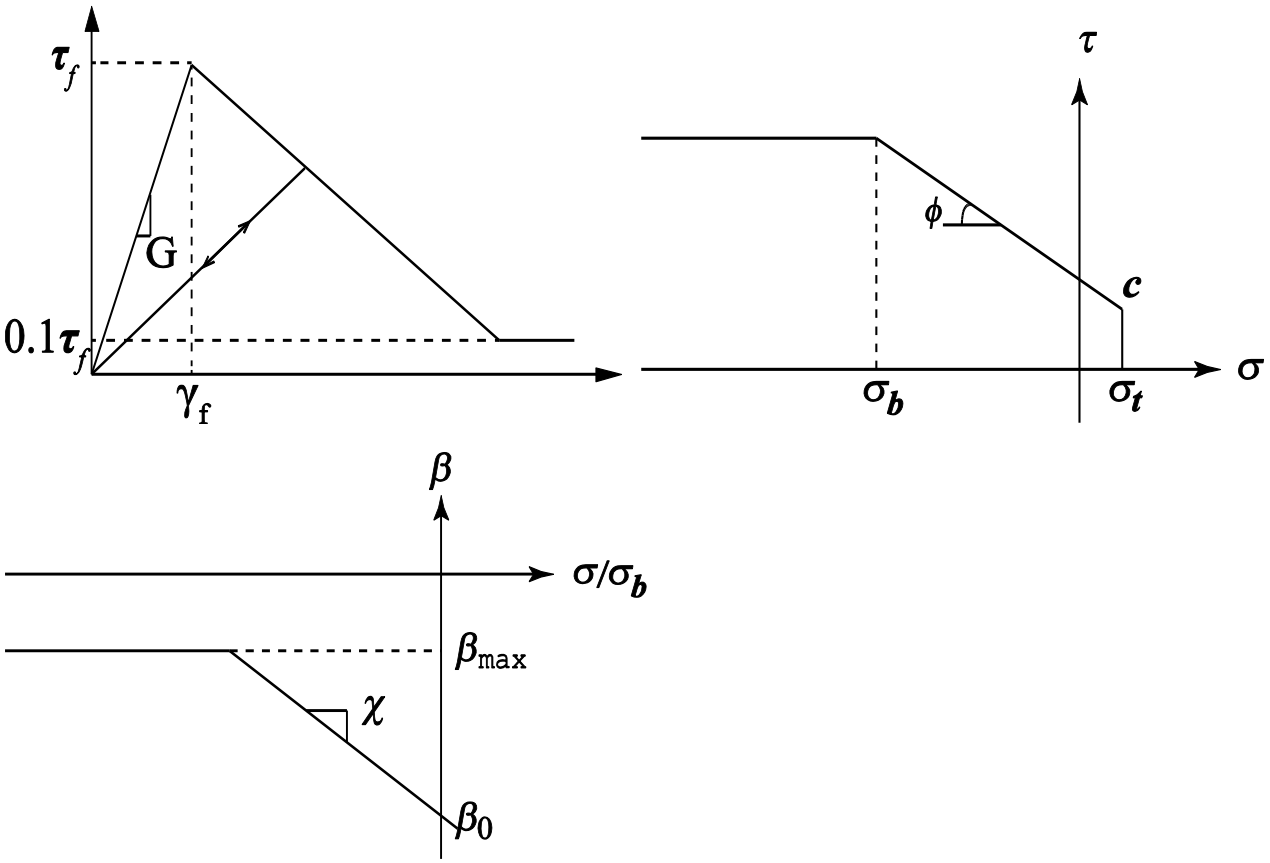

Fig. 16 Schematic shear springs in the mortar.

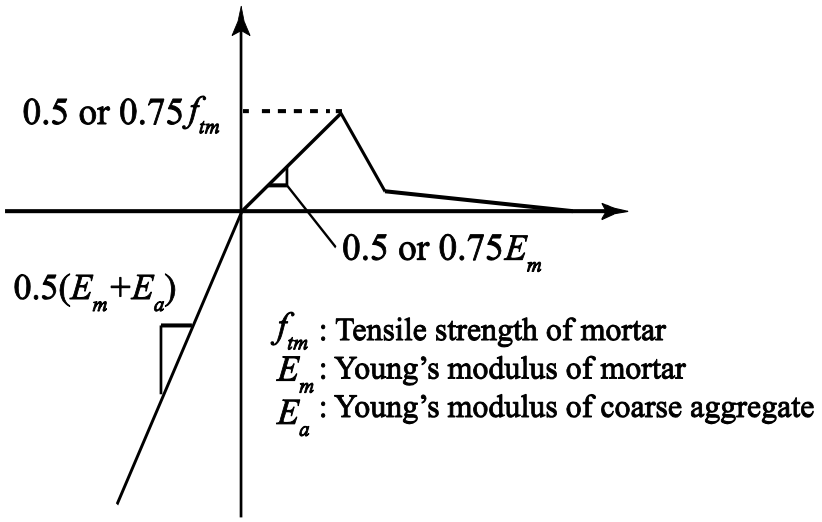

Fig. 17 Schematic of different properties of the ITZ in compression or tension fields.

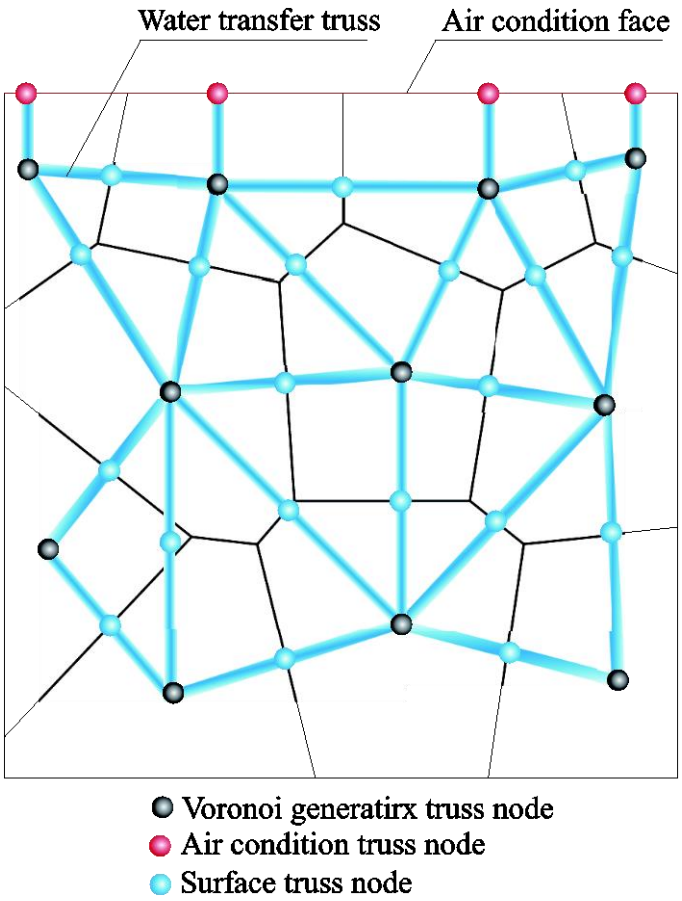

Fig. 18 Schematic of the truss network model for moisture transfer analysis.

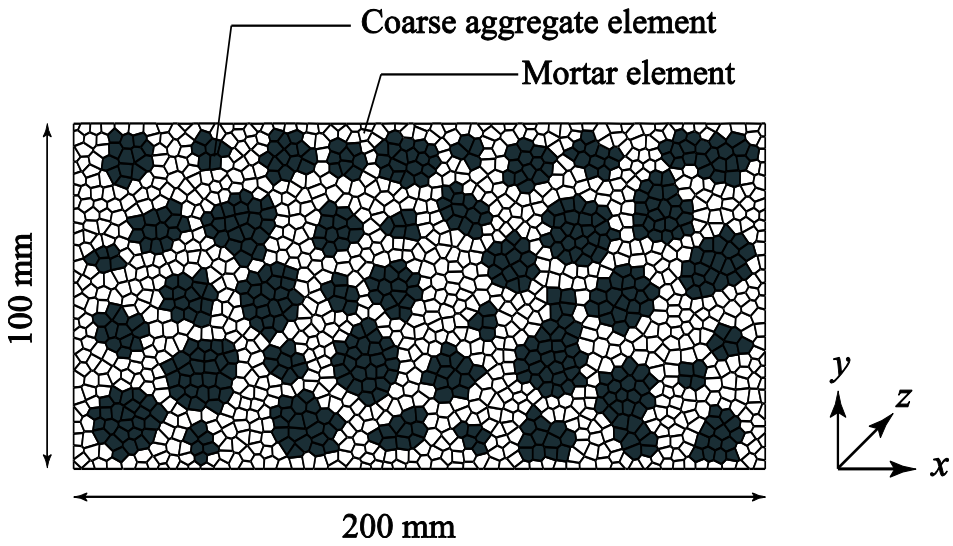

(a) Geometry of the meshing

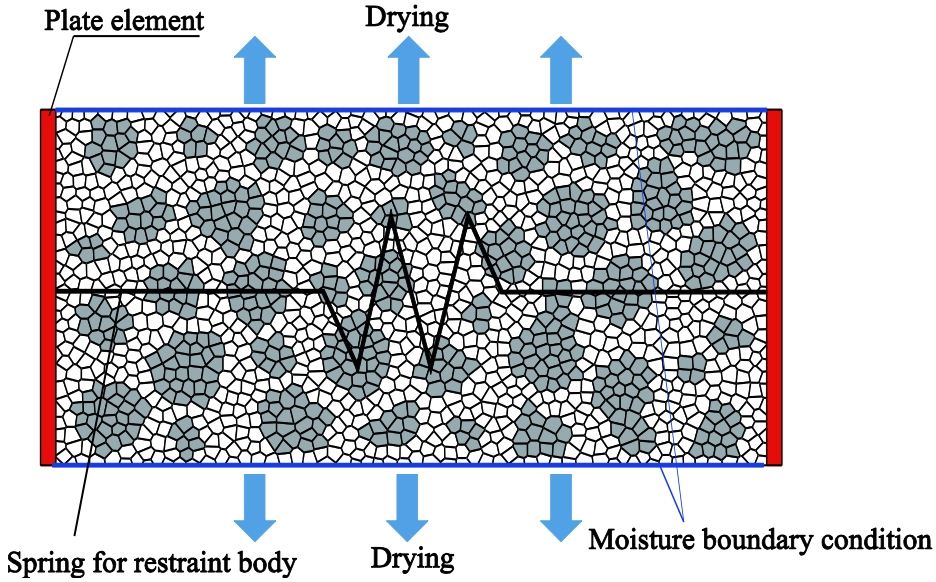

(b) Boundary conditions of the model.

Fig. 19 Meshing and boundary conditions.

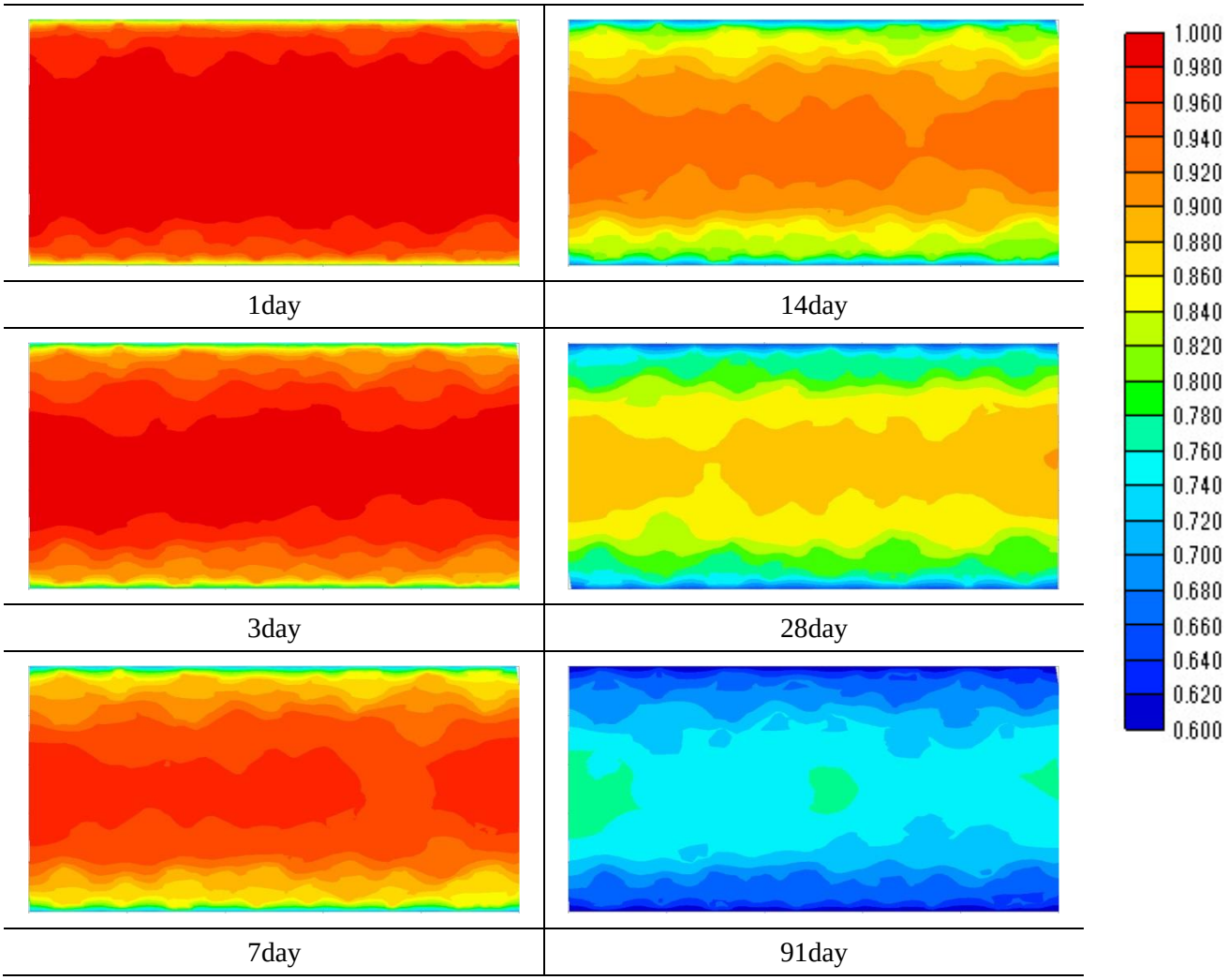

Fig. 20 Counter plots of the specimen as a function of equilibrium relative humidity.

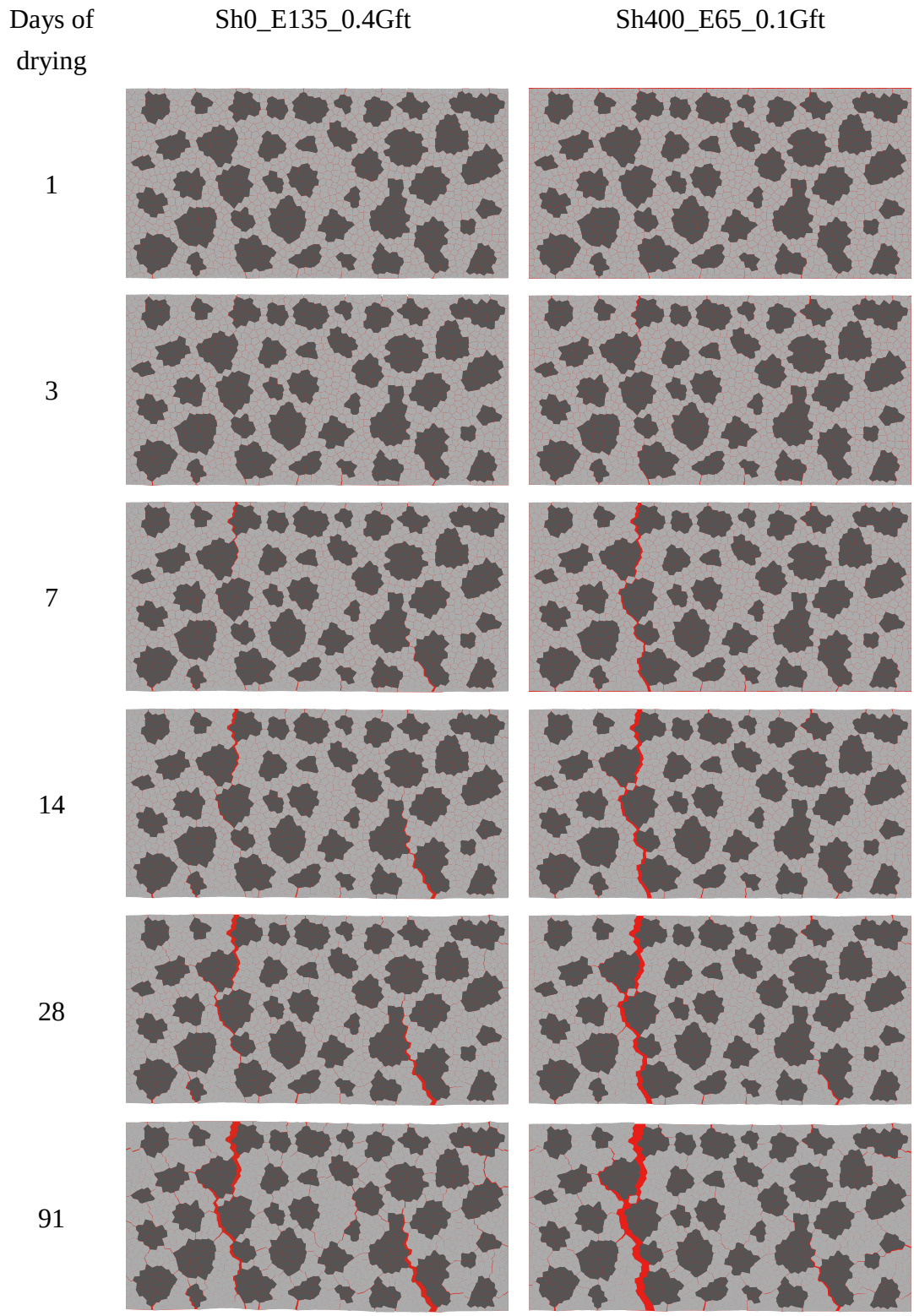

Fig. 21 Calculation results of Sh0_E135_0.4Gft and Sh400_E65_0.1Gft at different ages during drying. The width of the red line is linearly proportional to the tensile strain of normal spring. The magnification is 40x.

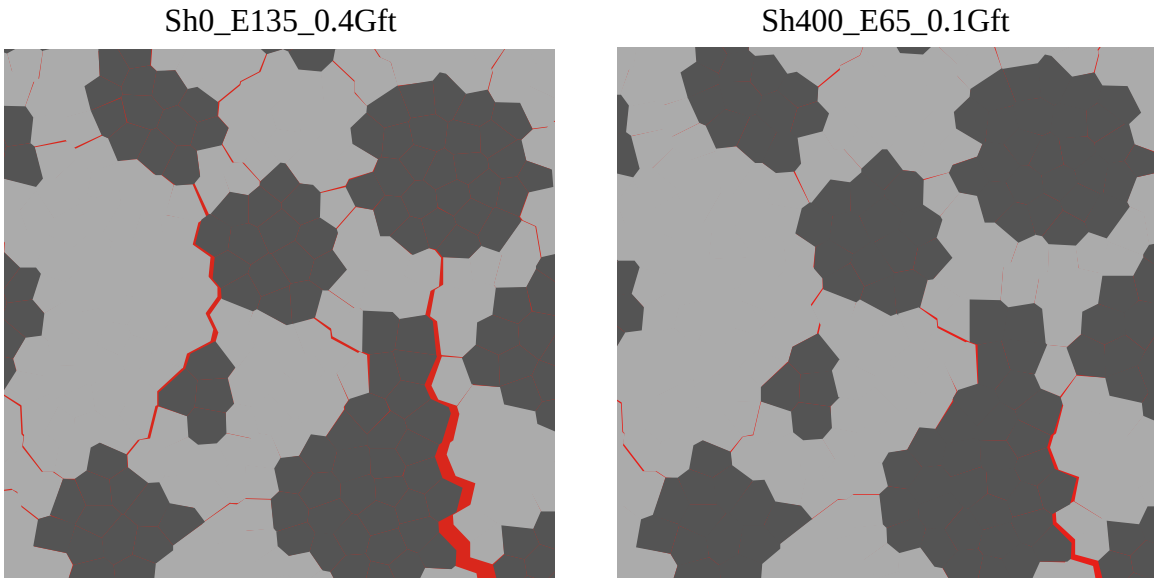

Fig. 22 Close-up of the cracking pattern around the aggregate at 91 days of drying in the calculation results of Sh0_E135_0.4Gft and Sh400_E65_0.1Gft.

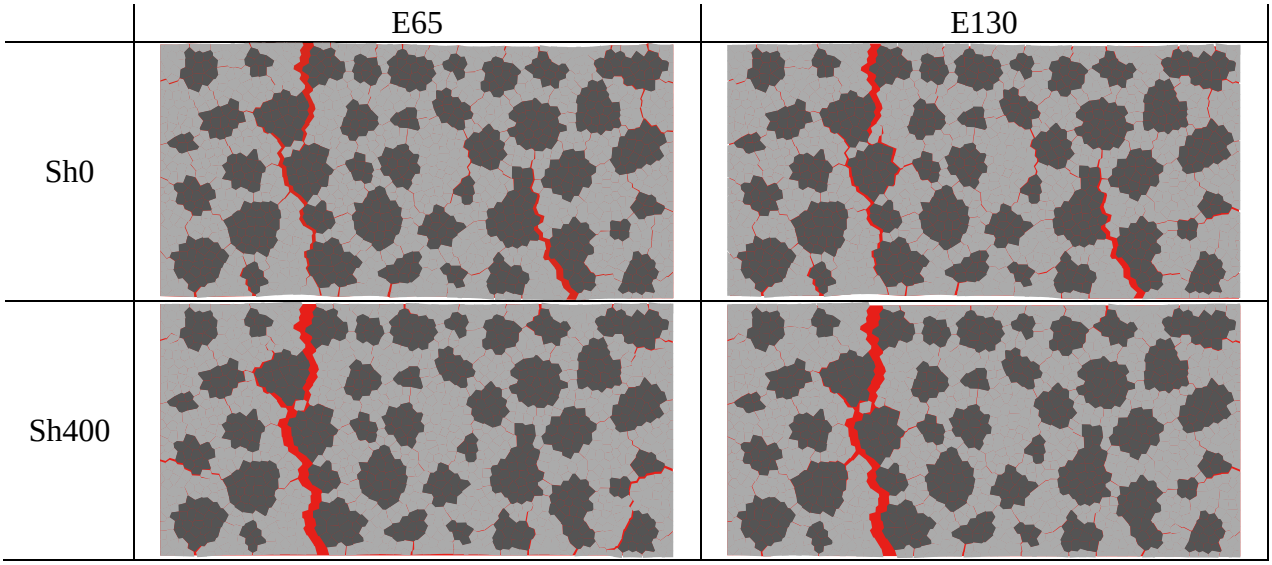

Fig. 23 Impact of shrinkage and Young's modulus of the aggregate on crack patterns in concretes. Sh0 and Sh400 depict aggregates having shrinkages of 0 and 400 microns, respectively. E65 and E130 depict aggregates having Young's moduli of 65 and 130 GPa, respectively.

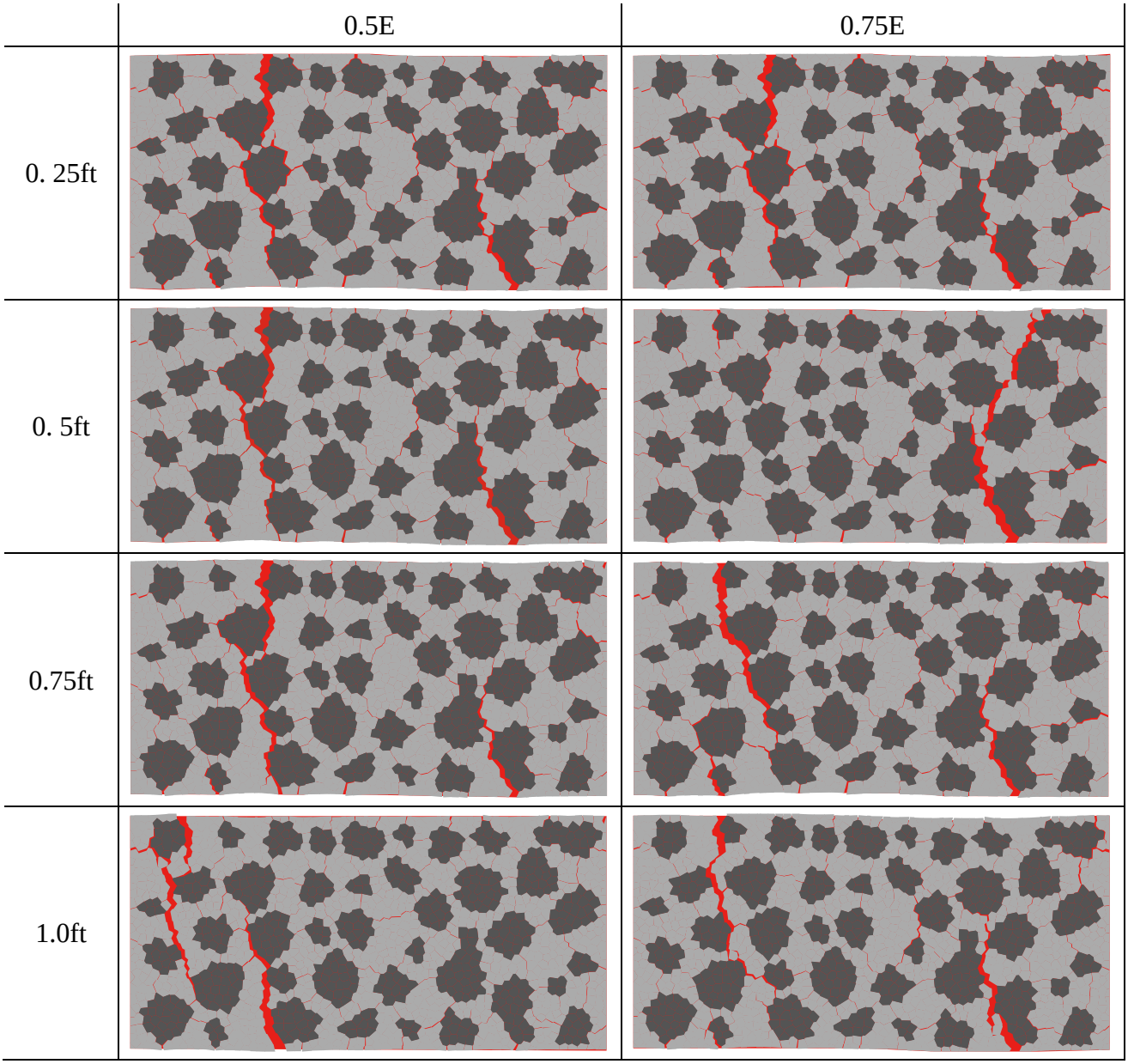

Fig. 24 Impact of strength and Young's modulus of the ITZ on crack patterns in concretes. 0.5E and 0.75E represent the Young's modulus of the ITZ, which equate to 0.5 and 0.75 times the Young's modulus of mortar. 0.25, 0.5ft, 0.75ft, and 1.0ft represent the strength of the ITZ, which equate to 0.25, 0.5, 0.75, and 1.0 times the strength of mortar.

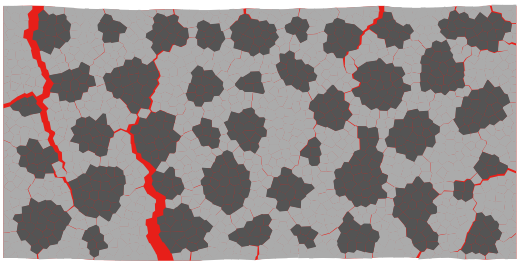

Sh0_0.1Gft

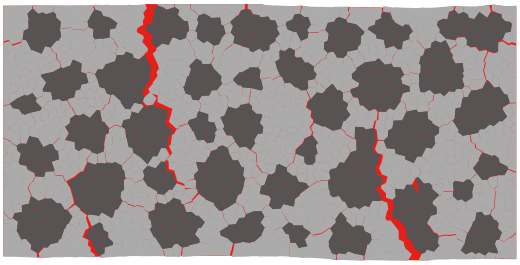

Sh0_0.2Gft

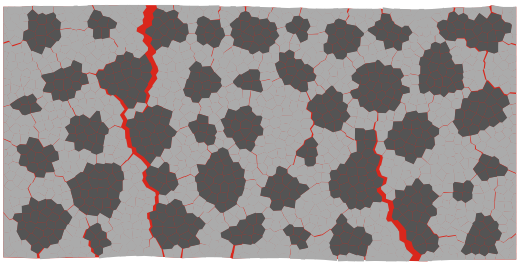

Sh0_0.4Gft

Fig. 25 Impact of fracture energy of ITZ on crack patterns in concretes.

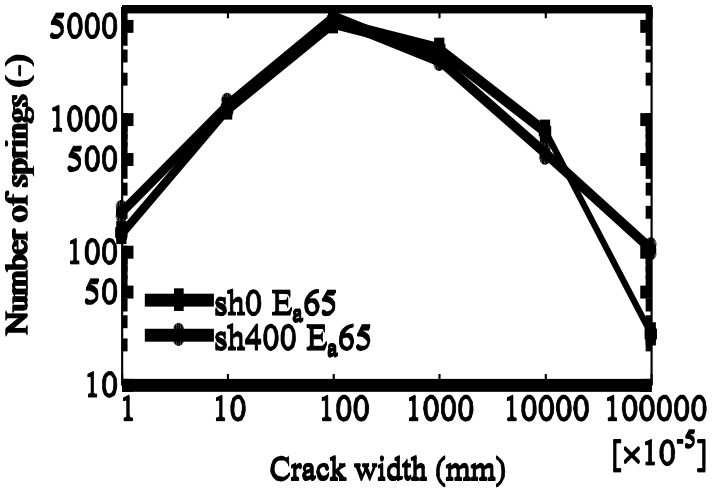

(a) Impact of aggregate shrinkage

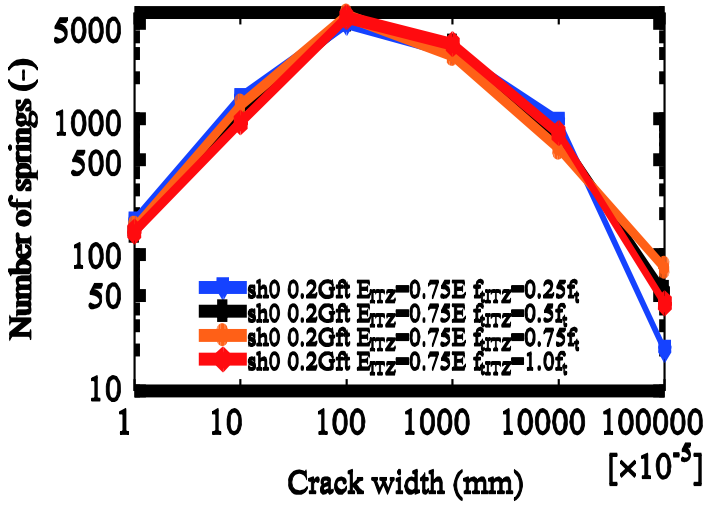

(b) Impact of strength of ITZ

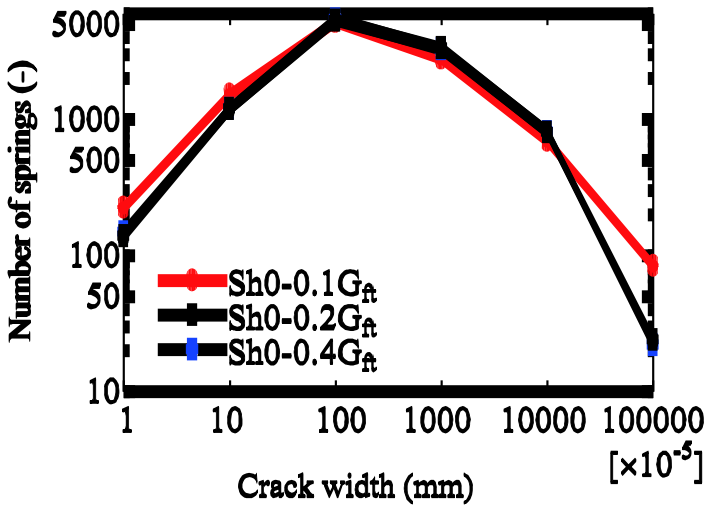

(c) Impact of fracture energy of ITZ

Fig.26 Crack distribution affected by (a) aggregate shrinkage and (b) fracture energy of ITZ.

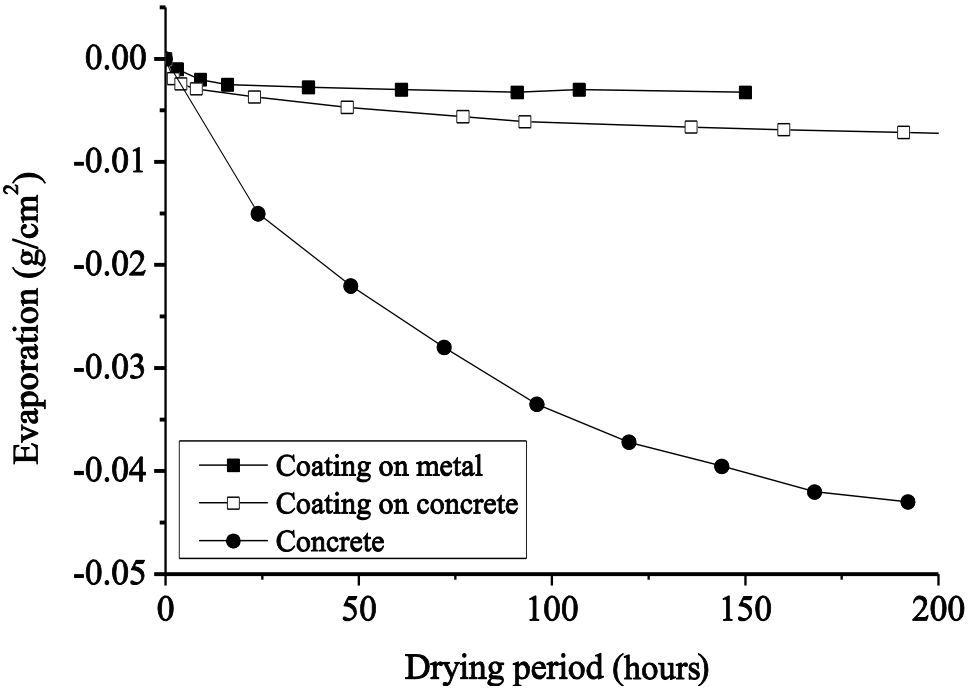

Fig. A-1 Water vapor evaporation from the surface of concrete or coating on concrete. Result of coating on metal is also shown for comparison. This indicates that coating material itself is dried under drying condition.